Vibrational level population of nitrogen impurities in low-pressure argon glow discharges†

Péter Simon* and Annemie Bogaerts

Received 6th October 2010, Accepted 12th November 2010
DOI: 10.1039/c0ja00179a

The vibrational level populations of the electronic ground state of the nitrogen molecule have been calculated for typical glow discharge conditions in argon–nitrogen mixtures with nitrogen concentrations between 0.1 and 1%. Stationary solutions of the master equations of the vibrational levels have been obtained using numerical methods. The main mechanisms responsible for the population and depopulation of the vibrational levels, and for the overall shape of the vibrational distribution function are pointed out. It has been found that vibration–vibration collisions play only a minor role and therefore the population of the vibrational levels is basically determined by the electron temperature.

Introduction

In the last decade a large amount of experimental data have been published on the effects of small concentrations of molecular gases (such as H_2, N_2, and O_2) present in Grimm-type glow discharges used for analytical purposes in glow discharge optical emission spectrometry (GD-OES).[1–8] Significant changes in the electrical characteristics, sputtering rates and in the relative intensities of emission lines were reported even at very low concentrations of molecular gases.[1–8] Despite some attempts[8] at explaining some of the experimental data, our understanding of the processes taking place in the presence of molecular gases is still far from complete.

Previously one of the authors (A.B.) developed a two-dimensional hybrid Monte Carlo-fluid model for investigating the effects of nitrogen addition to argon glow discharges.[9] Although this model included several ionized and electronically excited states of nitrogen, the vibrationally excited levels were omitted, in order not to further complicate the plasma chemistry. It is, however, well-known that these levels play a very important role in discharges containing high concentrations of nitrogen.[10,11] Therefore, the aim of the present study is to investigate whether the vibrational levels also play an important role in Ar glow discharges with only small concentrations of nitrogen. Moreover, we hope to obtain more insight into the mechanisms controlling the populations of the vibrational levels at these low nitrogen concentrations.

Description of the model

Only vibrational levels of the electronic ground state ($X^1\Sigma_g^+$) of N_2 are included in the model, and not the vibrational levels of the electronic excited states, as previous model calculations[9] have predicted that these excited levels have clearly lower densities than the ground state N_2 density. Several sets for the vibrational levels of $N_2(X^1\Sigma_g^+)$ exist in the literature. Depending on the choice of the potential and the methods used for the derivation, these sets may differ from each other not only in the exact value of the energies, but in the number of the levels as well. A short overview about the most often used sets can be found in ref. 12.

According to ref. 13 and 14 we consider 68 vibrational levels ($v = 0, 1, \ldots, 67$) of the $X^1\Sigma_g^+$ state of the nitrogen molecule. In Fig. 1 the energy of these levels is plotted. The energy of the vibrational ground state ($v = 0$) is 0.147 eV, the first vibrationally excited state lies above the ground state by 0.289 eV having an energy of 0.436 eV, while the last bound vibrational level below the dissociation limit ($v = 67$) has an energy of 9.911 eV. The master equations of these levels, describing the rate of change in the vibrational populations, are written as follows:

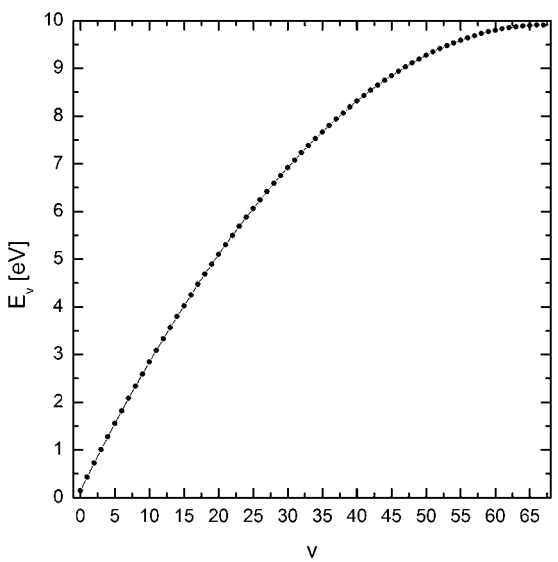

Fig. 1 Energy of the vibrational levels of the nitrogen electronic ground state, $N_2(X^1\Sigma_g^+)$.[13,14]

Research group PLASMANT, Department of Chemistry, Faculty of Sciences, University of Antwerp, Universiteitsplein 1, 2610 Wilrijk-Antwerp, Belgium. E-mail: peter.simon@ua.ac.be

† This article is part of a themed issue highlighting the latest work in the area of Glow Discharge Spectroscopy, including work presented at the International Glow Discharge Spectroscopy Symposium 2010, August 22–25, Albi, France.

$$\frac{dn_v}{dt} = \left(\frac{dn_v}{dt}\right)_{e-V} + \left(\frac{dn_v}{dt}\right)_{V-V} + \left(\frac{dn_v}{dt}\right)_{V-T}^{N_2} + \left(\frac{dn_v}{dt}\right)_{V-T}^{Ar} \quad (1)$$

where n_v denotes the density of level v and the terms on the right hand side represent the changes of the density due to

- electron impact excitation and de-excitation (e–V),
- vibration–vibration (V–V) and vibration–translation (V–T) energy exchange processes in N_2–N_2 collisions,
- vibration–translation (V–T) energy exchange processes in N_2–Ar collisions.

These processes are summarized in Table 1.

The rate coefficients of the e–V processes have been calculated using the cross-sections suggested by Phelps and Pitchford.[15] This set of cross-sections contains electron impact excitations from the vibrational ground state ($v = 0$) to the first eight vibrationally excited states ($v = 1$–8). In order to adjust these cross-sections to the specific energy levels used in the model, we have modified them in two steps. In the first step we have generated eight basic functions (β_v) by shifting the original cross-sections (σ_v) by their threshold energies (Δ_v):

$$\beta_v(\varepsilon) = \sigma_v(\varepsilon + \Delta_v).$$

Each of these basic functions corresponds to a transition by a specific number of quanta (from 1 to 8). Then in the second step we have created our own cross-sections by shifting these basic functions by the new threshold energies calculated from the energy level set:

$$\sigma_{vw}(\varepsilon) = \beta_{w-v}[\varepsilon - (E_w - E_v)],\ 1 \le w - v \le 8$$

where σ_{vw} is the cross-section of the electron impact excitation from level v to level w, and E_v and E_w denote the energies of the corresponding levels. Note that using this method we have been able to extend the cross-sections to any vibrational excitation with transitions up to 8 quanta.

The rate coefficients of the e–V processes are then given by

$$k_{vw}^{e-V} = \int_0^\infty \sigma_{vw}(\varepsilon) f_e(\varepsilon) \sqrt{2\varepsilon/m_e}\, d\varepsilon \quad (2)$$

where m_e is the mass of the electron and f_e is the electron energy distribution function (EEDF) normalized as

$$\int_0^\infty f_e(\varepsilon) d\varepsilon = 1$$

The rate coefficients of the de-excitation processes have been obtained by using the principle of detailed balance.

The V–V and V–T rate coefficients have been calculated by the Forced Harmonic Oscillator (FHO) model developed by Adamovich *et al.*[16] In V–V collisions only symmetric quantum transitions are included, however, multiquantum jumps up to 3 quanta are allowed both in V–V and V–T collisions as the energies of the levels with high quantum numbers lie very close to each other.

Table 1 Processes included in the model

$e^- + N_2(X,v) \rightleftharpoons e^- + N_2(X,w)$	e-V
$N_2(X,v) + N_2(X,w) \rightleftharpoons N_2(X,v+s) + N_2(X,w-s)$	V-V
$N_2(X,v) + N_2 \rightleftharpoons N_2(X,w) + N_2$	V-T
$N_2(X,v) + Ar \rightleftharpoons N_2(X,w) + Ar$	V-T

The vibrational level populations are calculated with a zero-dimensional model, hence assuming a uniform plasma. The parameters of the model are the temperature, the pressure and the ionization degree of the gas, the concentration of the nitrogen molecules and the temperature of the electrons. The first two parameters determine the density of the gas, the electron density can be calculated through the ionization degree while the density of nitrogen is given through its concentration. The gas temperature is used for calculating the V–V and V–T rate coefficients, the electron temperature with an assumed Maxwell–Boltzmann energy distribution gives the e–V rate coefficients through eqn (2).

Starting with an initial distribution where all the N_2 molecules are in the vibrational ground state, the densities of the vibrational levels are evolved in small time steps according to the master equations (eqn (1)). Once the steady state distribution is reached the densities remain constant.

Results and discussion

In glow discharges the input parameters of the model (gas temperature, electron density, electron temperature *etc.*) depend on the specific conditions, and may have a large variety of values and usually vary in space as well. For Grimm-type glow discharges some experimental values can be found in ref. 17–19 and values calculated by numerical models were presented in ref. 9 and 20. The zero-dimensional model presented in the previous section is certainly not able to accurately describe non-uniform plasmas as it neglects any transport phenomenon, but, for the same reason, the results of the model can be interpreted much easier and it can provide a good estimation for the populations of the vibrational levels. In the following discussion, one of our primary aims is therefore to give some general clues about how the population of the vibrational levels is affected by the different discharge parameters. The actual values used in the present study have been selected from ref. 9 and 20.

Stationary solutions of the master equations are calculated for two gas temperatures (T_g): 400 and 800 K. The corresponding pressures are chosen to be 400 and 800 Pa. Note that by using these parameters, the gas density remains unchanged. Two values are used for the ionization degree (α) of the gas: 10^{-7} and 10^{-5}, which correspond to an electron density of 7.24×10^9 cm^{-3} and 7.24×10^{11} cm^{-3}, respectively. The nitrogen concentration (c) is varied between 0.1 and 1%, while the electron temperature (T_e) is varied between 0.1 and 1 eV.

Calculated vibrational distribution functions (VDFs)

Fig. 2 shows the vibrational distribution functions (VDFs, *i.e.*, fraction of the population against vibrational energy of the various levels) at $T_g = 800$ K, $\alpha = 10^{-5}$, $c = 0.5\%$ but at different electron temperatures. It is obvious that the VDF drops much faster as a function of vibrational energy at the lowest values of T_e, which is like expected because the average electron energy (or

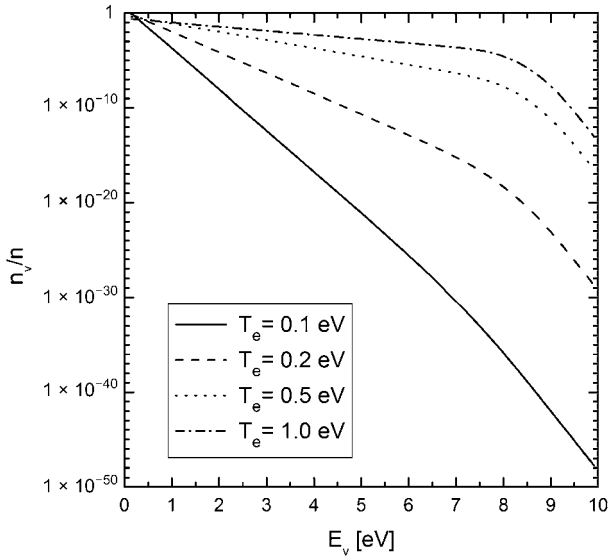

Fig. 2 VDFs for different electron temperatures at $T_g = 800$ K, $\alpha = 10^{-5}$ and N_2 concentration of 0.5%.

the fraction of high-energy electrons) is too low to populate the higher vibrational levels. When T_e is 0.1 eV, roughly only the vibrational ground state is populated. Indeed, the population of the third vibrational level (with energy around 1 eV) is already five orders of magnitude lower than the ground state population, and the levels around 5 eV (*i.e.*, $v \approx 20$) are more than 20 orders of magnitude lower in population than the ground state. For higher values of T_e, the VDF does not exhibit such a steep drop, as a larger fraction of electrons can populate the highly excited vibrational levels. Indeed, when T_e is equal to 1 eV, the population of the third vibrational level (with energy around 1 eV) is only one order of magnitude lower than the ground state population, and the levels around 5 eV (*i.e.*, $v \approx 20$) are about three orders of magnitude lower in population than the ground state. Further it is clear that each VDF starts with a straight line that holds until a transition region of about 8 eV and finally ends with another straight line. Linear fittings to the initial and final parts of the VDFs show that the low-lying vibrational levels are in equilibrium with the electrons at temperature T_e, while the high-lying levels are in equilibrium with the background gas at T_g.

This is a quite general feature of the VDFs. Indeed, it also holds for the graphs of Fig. 3 where results are presented for both gas temperatures (400 and 800 K) using different concentrations (0.1 and 1%) and different ionization degrees (10^{-7} and 10^{-5}). This behaviour of the VDF can be explained as follows: the low-lying levels are separated from each other by higher energy differences, and only the electrons have enough energy to be able to make transitions between these low-lying levels; at the higher vibrational levels, however, where vibrational transitions can be made with much less energy, the V–T collisions become dominant due to the high gas density. This also explains the effect of changing T_g or α: by decreasing the gas temperature or increasing the ionization degree (hence: the electron density) the transition from the e–V dominated part to the V–T dominated part of the VDF takes place at a higher energy level (see Fig. 3).

Although the graphs of Fig. 3(a) and (b) look quite similar, a small but interesting difference can be spotted: at $\alpha = 10^{-7}$ in

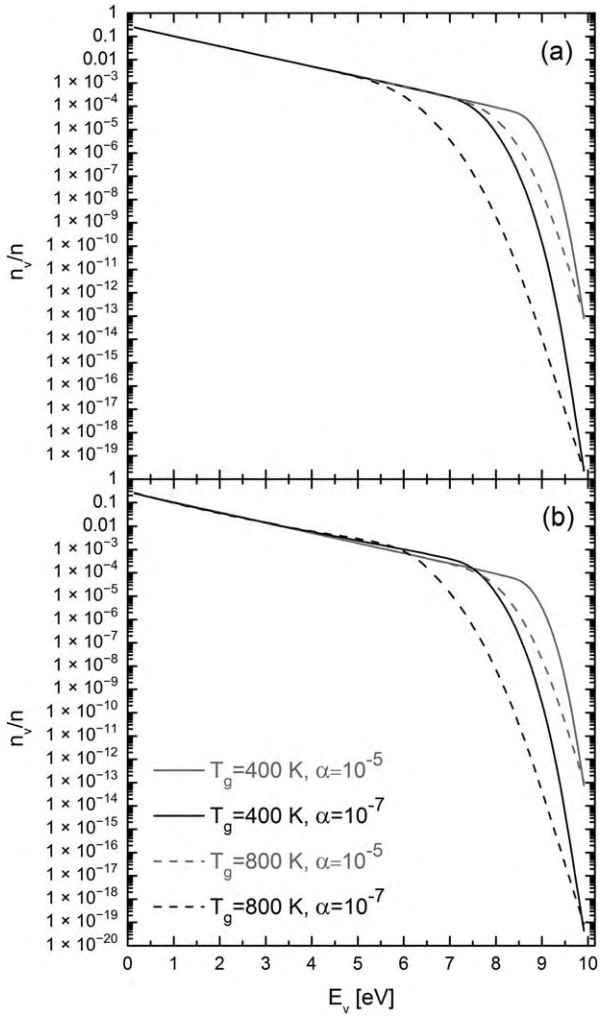

Fig. 3 VDFs for different gas temperatures and ionization degrees at $T_e = 1$ eV and N_2 concentrations of (a) 0.1%, (b) 1%.

figure (b) (*i.e.*, 1% N_2 concentration) the populations of the vibrational levels at around 6 eV slightly exceed the values that would correspond to a Boltzmann distribution at temperature T_e; this behaviour is, however, absent in figure (a) (*i.e.*, 0.1% N_2 concentration).

This deviation is made more clear in Fig. 4(a) where the ratios of the VDFs of higher nitrogen concentrations to the VDF at nitrogen concentration of 0.1% are plotted. The higher the nitrogen concentration, the larger is the deviation from the population distribution at 0.1% N_2 concentration. More specifically, a minor increase is seen for the lowest vibrational levels, a slight drop for the levels between 1 and 2 eV, and a significant increase for the levels above 4 eV (and more in particular above 7 eV). In Fig. 4(b) the total net V–V production rates of the vibrational levels, divided by the total nitrogen density, are shown. Note that the negative values of R_{VV} represent a net loss of these levels by V–V collisions, whereas positive values indicate a net production of these levels. Hence, V–V processes populate the lowest vibrational levels, depopulate the levels in the energy range of about 1 and 2 eV, and populate again the higher levels. By increasing the N_2 concentration this effect of the V–V collisions becomes more pronounced. The correlation between the

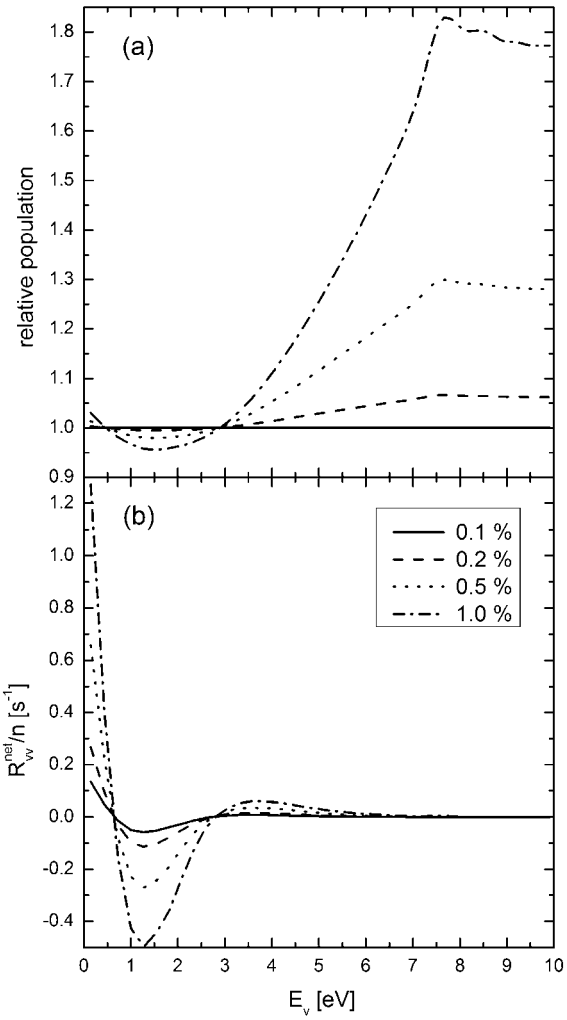

Fig. 4 (a) Ratios of the VDFs to the VDF at N_2 concentration of 0.1%. (b) Total net V–V production of the vibrational levels divided by the total N_2 density ($T_e = 1$ eV, $T_g = 400$ K, and $\alpha = 10^{-7}$).

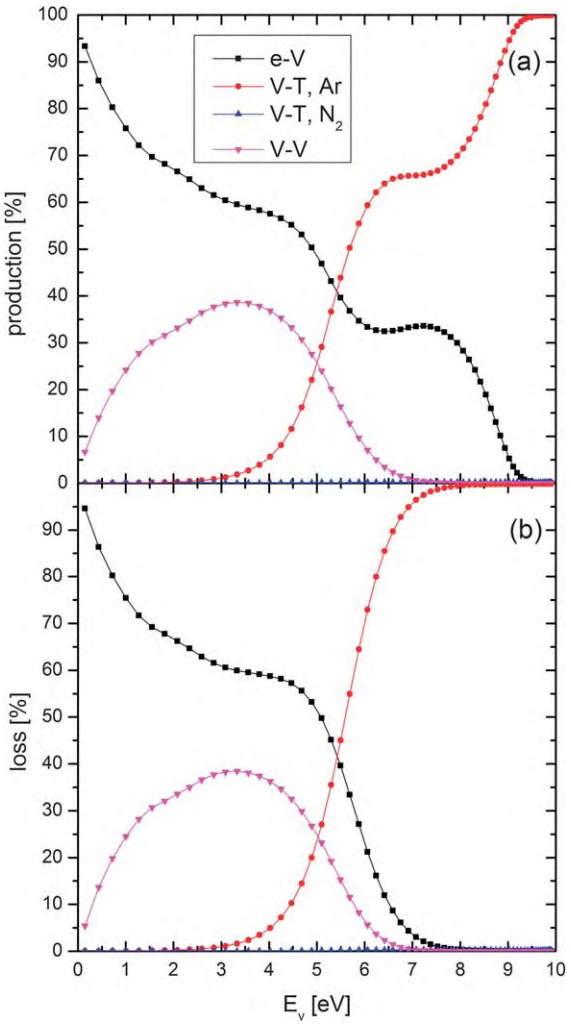

Fig. 5 Relative contributions of the different types of processes to the production (a) and loss (b) of the vibrational levels at N_2 concentration of 0.1%, $T_e = 1$ eV, $T_g = 800$ K and $\alpha = 10^{-7}$.

graphs of the two subfigures of Fig. 4 provides a clear evidence that the pumping-up mechanism[21] of the V–V processes is responsible for the above mentioned deviations in the populations.

Although the minimum at about 1.5 eV and the fast increase until 7.5 eV in the relative populations of the VDFs in Fig. 4(a) can easily be explained by the effect of the V–V collisions, the origin of the slow decrease above 7.5 eV is not so evident. By increasing the concentrations of nitrogen, this decrease becomes more pronounced. In fact this region is already dominated by the V–T collisions (see Fig. 3) and this behaviour is due to the fact that the rate coefficients of the V–T collisions are a bit higher in the case of N_2 than in the case of Ar.

Importance of the various production and loss processes for the vibrational levels

Fig. 5 and 6 show the relative contributions of the e–V, V–V and the V–T processes (both with Ar and with N_2) to the production (subfigures (a)) and loss (subfigures (b)) of each vibrational level. The corresponding parameters are as follows: $T_g = 800$ K, $\alpha = 10^{-7}$, $T_e = 1$ eV and the N_2 concentration is 0.1% for Fig. 5 and 1% for Fig. 6. As expected the e–V and V–V collisions dominate the production and loss processes of the low-lying levels while the high-lying levels interact mostly through V–T collisions with Ar. The V–T collisions with N_2 are more or less negligible, as expected because the N_2 concentration is only 0.1% or 1% of the Ar concentration. It is worth mentioning that while in the case of 0.1% N_2 concentration the e–V collisions give the major contribution to the production and loss processes of the low-lying levels, in the case of 1% N_2 concentration the major role is played by the V–V processes. We have pointed out during the analysis of Fig. 3 and 4 that this difference is reflected in the shape of the VDFs as well.

Electron energy loss due to vibrational (and rotational) excitation

It is observed that mostly the same types of collisions are responsible for both the production and the loss of each vibrational state. However, the transition region from the e–V to the

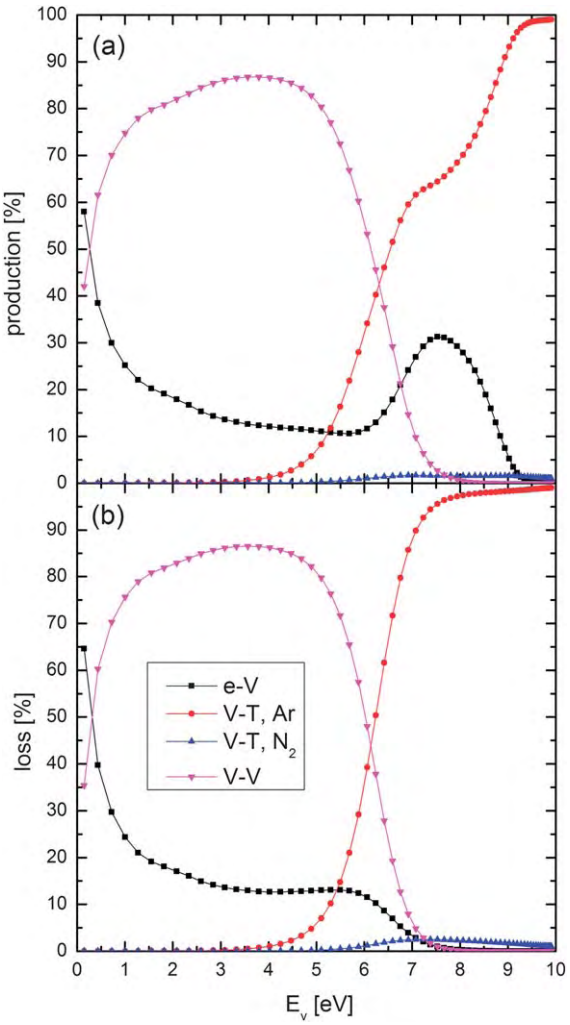

Fig. 6 Relative contributions of the different types of processes to the production (a) and loss (b) of the vibrational levels at N_2 concentration of 1%, $T_e = 1$ eV, $T_g = 800$ K and $\alpha = 10^{-7}$.

V–T dominated part of the VDF is an exception: the production due to e–V collisions is compensated by the loss due to V–T processes. The question is immediately raised: how much energy is transferred from the electrons to the background gas due to their interaction through the vibrational levels? In order to answer this question we have calculated this amount of energy and compared it with the energy loss due to rotational excitations.

The rate coefficients of rotational excitations are calculated in the same way as the vibrational ones, *i.e.* using eqn (2) and the rotational cross-section given in ref. 15. This cross-section was derived from gas-heating data using the single level approximation with an energy loss of 0.02 eV.

Fig. 7 shows the net energy loss of electrons in e–V and e–R collisions for four different electron temperatures at $T_g = 800$ K, $\alpha = 10^{-5}$ and N_2 concentration of 0.5%. Note that the net energy loss in e–V collisions is the difference between the energy loss in vibrational excitations and the energy gain in vibrational de-excitations. For the e–R collisions, we have assumed that the net energy loss is equal to the energy loss of electrons due to

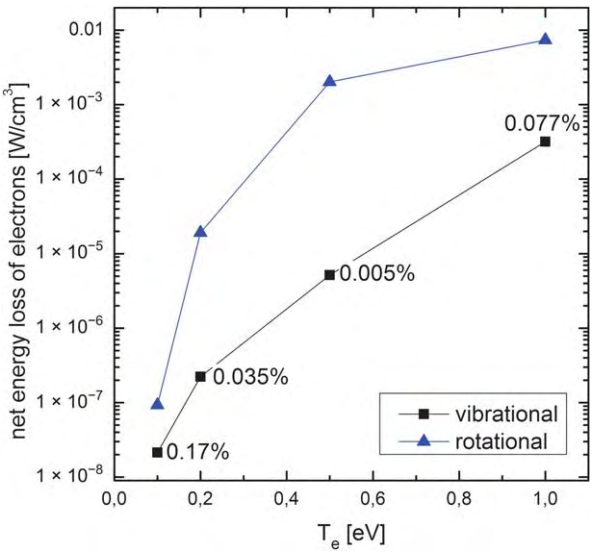

Fig. 7 The net energy loss of electrons in e–V and e–R collisions as a function of electron temperature at $T_g = 800$ K, $\alpha = 10^{-5}$ and N_2 concentration of 0.5%. The ratios of the net energy loss in e–V collisions to the absolute energy loss in vibrational excitations are indicated next to the symbols.

rotational excitations. Indeed, the number of collisions required for the relaxation of the rotationally excited states to the gas temperature in nitrogen is about 4 at 400 K and remains in the order of 10 below 1500 K.[22] Effective rotational–translational (R–T) relaxation between N_2 and Ar often makes it possible to determine the temperature of the argon gas by measuring the rotational temperature of the N_2 molecules (see *e.g.* ref. 23). Based on these facts, we have assumed that de-excitation processes are negligible and that the net energy loss is equal to the energy loss due to excitation.

The energy loss in e–R collisions is about 1 or 2 orders of magnitude higher than in e–V collisions throughout the whole electron temperature range. A significant increase in the energy loss is observed going from low to high electron temperatures. In the case of rotational levels this increase is simply due to the higher rate coefficients. In the case of vibrational levels, several factors play a role. Most of these factors, however, can be traced back to the increase in the population of higher vibrational levels (Fig. 2).

The numbers next to the symbols of the vibrational curve of Fig. 7 show the ratios of the net energy loss of electrons in e–V collisions to their absolute energy loss in vibrational excitations. It is clear that more than 99% of the energy lost in vibrational excitation is gained back *via* de-excitation collisions.

Fig. 8 shows the net energy loss of electrons in e–V and e–R collisions for four different N_2 concentrations at $T_e = 1$ eV, gas temperatures of 400 and 800 K and ionization degrees of 10^{-7} (figure (a)) and 10^{-5} (figure (b)). The numbers next to the symbols in Fig. 8 have the same meaning as in Fig. 7. As the electron temperature is fixed now, the behaviour of the energy loss in e–R processes is easy to understand: the rate of rotational excitations, and therefore the energy loss, is proportional both to the electron and to the nitrogen density. Hence the values of the rotational curve in figure (a) are 100 times less than in figure (b) and these

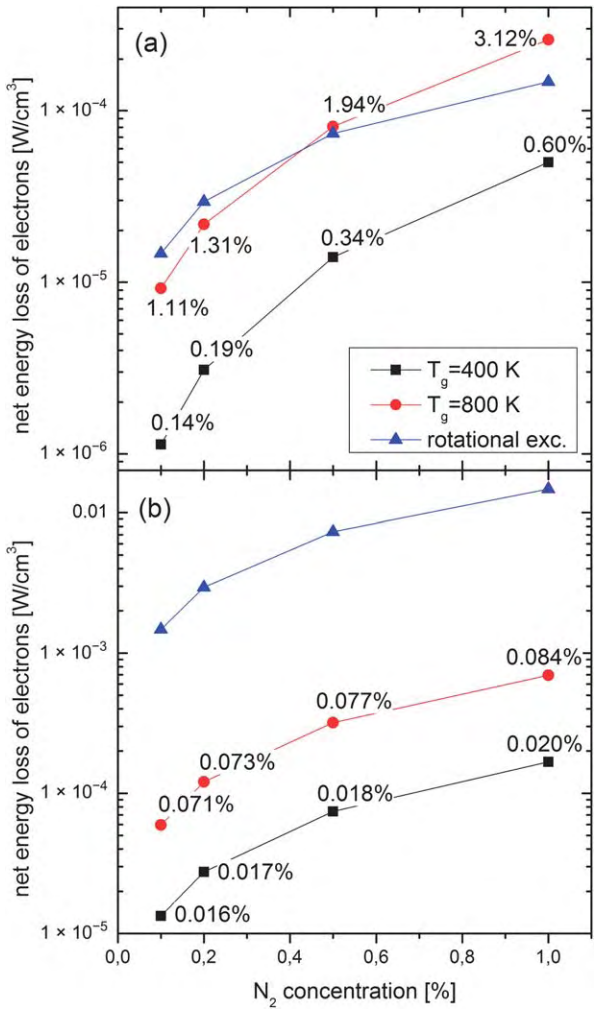

Fig. 8 The net energy loss of electrons in e–V and e–R collisions as a function of N_2 concentration for different gas temperatures at $T_e = 1$ eV and ionization degree of (a) 10^{-7} and (b) 10^{-5}. The ratios of the net energy loss in e–V collisions to the absolute energy loss in vibrational excitations are indicated next to the symbols.

graphs can be used to find linear behaviour on a logarithmic scale.

The energy loss of electrons in e–V collisions at 800 K is significantly higher than at 400 K. This is due to the fact that at higher temperature the V–V and V–T rate coefficients are higher (except for the very high vibrational levels), and therefore there is an interaction with the more populated intermediate levels as well. The vibrational curves in figure (b) run parallel to the rotational curve, which means that they grow linearly with the N_2 concentration, while the vibrational curves of figure (a) grow faster than linear and the one corresponding to 800 K exceeds the rotational curve at about 0.5% N_2 concentration.

Finally we would like to mention an example of high N_2 concentration for comparison. At $T_g = 800$ K, $T_e = 1$ eV, $\alpha = 10^{-7}$ and N_2 concentration of 90% the net energy loss of electrons in e–V and e–R collisions is 0.31 W cm^{-3} and 0.013 W cm^{-3}, respectively. The net energy lost in e–V collisions is 41% of the energy lost in vibrational excitations. We have repeated the simulation with the same parameters but leaving out the V–V collisions. In this case the net energy loss of the electrons in e–V collisions has been found to be 0.0012 W cm^{-3}, which is 0.16% of the energy lost in vibrational excitations. This example shows that V–V processes make the real difference between the low and high N_2 concentrations.

Conclusion

This paper intended to give a general insight into the mechanisms controlling the vibrational populations of nitrogen impurities in argon glow discharges. By using a simple model based on the master equations of the vibrational levels we have been able to shed light on the role played by the e–V, V–V and V–T processes and to give an idea on how the VDF is affected by the different discharge parameters.

It has been found that the electron temperature has the largest influence on the populations of the vibrational levels. Accurate electron temperatures are therefore necessary to get reliable VDFs. Although V–T processes control the high-lying vibrational levels, and therefore the shape of the high-energy part of the VDF, the overall populations of these levels are still basically determined by the electron temperature.

V–V collisions play an important role in discharges containing high concentrations of nitrogen as they have a large influence on the VDF and indirectly they can affect the electron temperature as well. However, at concentrations of interest for GD-OES they have much less significance.

Acknowledgements

This work has been supported by the European Marie Curie Research Training Network GLADNET, contract no. MRTN-CT-2006-035459. The authors would like to thank I. V. Adamovich for the helpful discussion on the FHO model.

References

1 V.-D. Hodoroaba, V. Hoffmann, E. B. M. Steers and K. Wetzig, *J. Anal. At. Spectrom.*, 2000, **15**, 951–958.
2 V.-D. Hodoroaba, V. Hoffmann, E. B. M. Steers and K. Wetzig, *J. Anal. At. Spectrom.*, 2000, **15**, 1075–1080.
3 K. Wagatsuma, *Spectrochim. Acta, Part B*, 2001, **56**, 465–486.
4 V.-D. Hodoroaba, E. B. M. Steers, V. Hoffmann, W. E. S. Unger, W. Paatsch and K. Wetzig, *J. Anal. At. Spectrom.*, 2003, **18**, 521–526.
5 P. Smíd, E. B. M. Steers, Z. Weiss and J. Vlcek, *J. Anal. At. Spectrom.*, 2003, **18**, 549–556.
6 E. B. M. Steers, P. Smíd and Z. Weiss, *Spectrochim. Acta, Part B*, 2006, **61**, 414–420.
7 E. B. M. Steers, P. Smíd, V. Hoffmann and Z. Weiss, *J. Phys.: Conf. Ser.*, 2008, **133**, 012020.
8 P. Smíd, E. Steers, Z. Weiss, J. Pickering and V. Hoffmann, *J. Anal. At. Spectrom.*, 2008, **23**, 1223–1233.
9 A. Bogaerts, *Spectrochim. Acta, Part B*, 2009, **64**, 126–140.
10 V. Guerra, P. A. Sá and J. Loureiro, *Eur. Phys. J.: Appl. Phys.*, 2004, **28**, 125–152.
11 P. A. Sergeev and D. I. Slovetsky, *Chem. Phys.*, 1983, **75**, 231–241.
12 M. Lino da Silva, V. Guerra, J. Loureiro and P. A. Sá, *Chem. Phys.*, 2008, **348**, 187–194.
13 G. Colonna, F. Esposito and M. Capitelli, *AIAA 2003-3645, 36th AIAA Thermophysics Conference*, Orlando, FL, 23–26 June 2003.
14 G. Colonna, D. D'Ambrosio and M. Capitelli, *AIAA 2007-3906, 39th AIAA Thermophysics Conference*, Miami, FL, 25–28 June 2007.
15 A. V. Phelps and L. C. Pitchford, *Phys. Rev. A: At., Mol., Opt. Phys.*, 1985, **31**, 2932–2949, http://jila.colorado.edu/~avp/collision_data.

16 I. V. Adamovich, S. O. Macheret, J. W. Rich and C. E. Treanor, *J. Thermophys. Heat Transfer*, 1998, **12**, 57–65.
17 N. P. Ferreira, H. G. C. Human and L. R. P. Butler, *Spectrochim. Acta, Part B*, 1980, **35**, 287–295.
18 M. Kuraica, N. Konjevic, M. Platisa and D. Pantelic, *Spectrochim. Acta, Part B*, 1992, **47**, 1173–1186.
19 A. Bogaerts, A. Quentmeier, N. Jakubowski and R. Gijbels, *Spectrochim. Acta, Part B*, 1995, **50**, 1337–1349.
20 A. Bogaerts, R. Gijbels and V. V. Serikov, *J. Appl. Phys.*, 2000, **87**, 8334–8344.
21 C. E. Treanor, J. W. Rich and R. G. Rehm, *J. Chem. Phys.*, 1968, **48**, 1798–1807.
22 C. Park, *J. Thermophys. Heat Transfer*, 2004, **18**, 527–533.
23 N. Britun, M. Gaillard, A. Ricard, Y. M. Kim, K. S. Kim and J. G. Han, *J. Phys. D: Appl. Phys.*, 2007, **40**, 1022–1029.

